Gel-Immobilized Colloidal Crystal Shell with Enhanced Thermal Sensitivity at Photonic Wavelengths

By *Toshimitsu Kanai, Daeyeon Lee, Ho Cheung Shum, Rhutesh K. Shah,* and *David A. Weitz**

Microcapsules are sub-millimeter sized core-shell structures that are often used for encapsulation applications. The shell not only protects the core materials but also imparts additional properties to the capsules. For example, shells have been made from various functional materials such as gels,[1] magnetic materials,[2] and liquid crystals[3] to impart desired mechanical strength, biocompatibility, permeability, and release properties to the microcapsules. Such microcapsules are often used for a variety of applications such as macromolecular delivery,[4] hazardous material handling,[5] oil recovery,[6] and food processing.[7] The choice of an appropriate shell material is important for the development of microcapsules with new functionalities for novel applications in pharmaceutical, food, cosmetic, and materials industries.

Charge-stabilized colloidal crystals are three-dimensional periodic arrays of charged particles with low packing density in a liquid medium.[8] The spatial periodicity of the refractive index of the colloidal crystalline arrays results in an optical stop band effect, and, hence, they act as photonic crystals in the optical regime.[9] Since the charged colloids do not touch one another, the lattice constant can be conveniently tuned by changing the particle volume fraction. The wavelength of the optical stop band can be fixed by immobilizing these crystals in a hydrogel.[10] The Bragg wavelength can be altered on-demand if a stimuli-sensitive hydrogel is used. By adjusting the volume of the hydrogel through an external stimulus, the lattice constant of the crystals can be tuned accordingly; this is useful for applications such as tunable photonic crystals,[11] tunable laser,[12] and biological and chemical sensors.[13] In particular, capsules with a shell of such colloidal crystals will enable labeling and monitoring of the encapsulated materials as well as the environment around the capsules through the wavelength of the optical stop band or diffraction color.

[*] H. C. Shum, Dr. R. K. Shah, Prof. D. A. Weitz
School of Engineering & Applied Sciences
and Department of Physics
Harvard University
Cambridge, MA 02138 (USA)
E-mail: weitz@seas.harvard.edu
Prof. T. Kanai
Department of Chemical and Energy Engineering
Yokohama National University
Yokohama, 240–8501 (Japan)
Prof. D. Lee
Department of Chemical and Biomolecular Engineering
University of Pennsylvania
Philadelphia, PA 19104 (USA)

DOI: 10.1002/adma.201002055

In this Communication, we demonstrate that monodisperse double emulsions with colloidal crystal shells can be fabricated through microfluidic techniques.[14] The colloidal crystal shells are subsequently immobilized in the hydrogel network by photo-polymerization techniques. The wavelength of the optical stop band of the gel-immobilized colloidal crystal shell can be adjusted by simply varying the particle concentration before polymerization. Moreover, it can also be altered by external stimuli, such as temperature, after preparation by using the stimuli-sensitive hydrogel. We also show that the gel-immobilized colloidal crystal shell has a higher sensitivity and wider range in the stop band wavelength than that displayed by a bulk gel.

Our microfluidic device combines co-flow and flow-focusing geometries to generate monodisperse oil-in-water-in-oil (O/W/O) double emulsions (**Scheme 1**). The inner oil phase is pumped through the tapered round capillary while the middle aqueous phase flows through the region between the inner round capillary and the outer square capillary in the same direction. The outer oil phase flows through the outer capillary in the opposite direction, and hydrodynamically focuses the inner and middle phases, which break up at the orifice of the collection tube to form monodisperse O/W/O double emulsions. The inner and outer oil phases are poly(dimethylsiloxane) oil (PDMS). The outer oil phase contains a surfactant (2 wt%, Dow Corning 749) to stabilize the interface between the middle aqueous and outer oil phase. The aqueous phase contains charged polystyrene particles. A surfactant (2.5 wt%, Tween 20) is also added to the aqueous phase to stabilize the interface between the middle aqueous and the inner oil phase. The quiescent particles are in a crystalline state in the aqueous phase and retain their crystallinity upon formation of double emulsion drops. In order to immobilize the colloidal crystals in the aqueous phase, gelation reagents that include a monomer, a cross-linker, and a polymerization initiator are added. The solutions are filtered and then injected into the microfluidic device. Double emulsion droplets with colloidal crystal shells are irradiated with UV light to photo-polymerize the middle phases, thus immobilizing the colloidal crystals in the hydrogel shells. We extract the PDMS oil from the microcapsules by washing with 2-propanol and then with water.

When the fabrication conditions, including the surfactant concentration, the gel-reagent concentration, and the particle concentration are not set appropriately, stable double emulsions with colloidal crystal shells cannot be obtained; for example, an insufficient amount of surfactant in the middle aqueous phase leads to coalescence of inner oil drop with the outer oil phase, whereas excess surfactant results in coalescence of middle

© 2010 WILEY-VCH Verlag GmbH & Co. KGaA, Weinheim

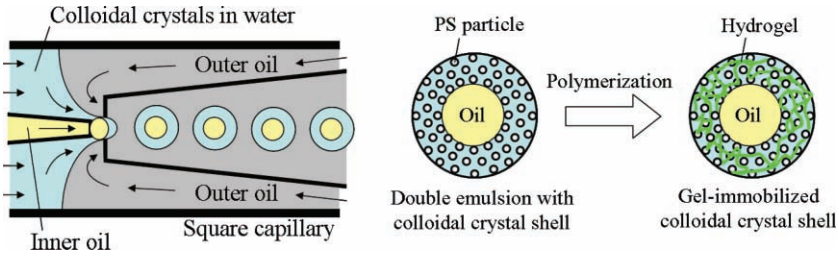

Scheme 1. Schematic of the procedures used for fabrication of microcapsules with gel-immobilized colloidal crystal shells using capillary microfluidics and photopolymerization. The aqueous phase is a suspension of charged polystyrene particles containing a surfactant and gelation reagents. The outer oil phase is a PDMS oil with a surfactant. The double emulsions formed with colloidal crystal shells are irradiated with UV light to polymerize the hydrogel and immobilize the loosely-packed colloidal crystals in the network, forming the colloidal crystal shells.

aqueous phases and destruction of crystalline structure of charged colloids. Under optimized conditions, however, stable double emulsions with colloidal crystal shells can be formed (**Figure 1a**). The double emulsion drops with colloidal crystal shells remain very stable and monodisperse, exhibiting diffraction color in the reflection microscopy image shown in Figure 1b. The observed color diffraction pattern of the shells is the same as that of the spherical colloidal crystals,[15] and is caused by the spherical shape and relatively high contrast between the refractive indices of the colloidal particles and the surrounding phase.[16] One of the most attractive features of microfluidic techniques is the precise control over the dimensions of the double emulsions. The size of the outer and inner drops, and thus the thickness of the colloidal crystal shell, can be tuned by changing the flow rates of each phases and/or the size of the capillary orifices. For example, double emulsions with thinner colloidal crystal shells and larger inner drops are formed by gradually decreasing the flow rate of the middle phase (Figure 1c–f). Furthermore, the number of drops encapsulated in the colloidal crystal shell can be manipulated by adjusting the flow rates (see supporting information).

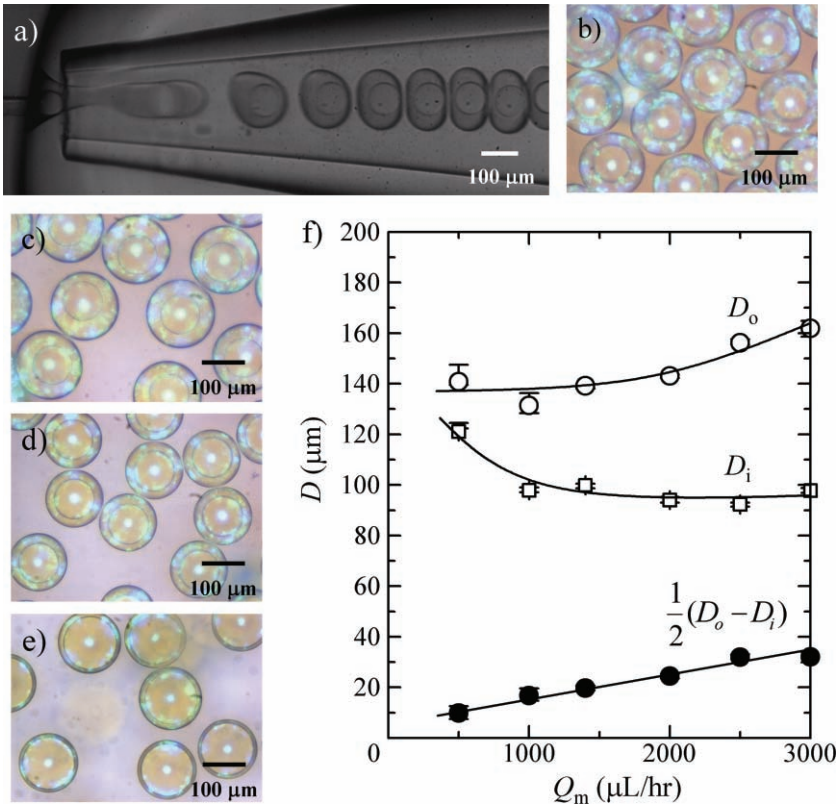

Figure 1. a) Formation of double emulsions with colloidal crystal shells in the microfluidic device. The diameter of the polystyrene colloids is 120 nm. The flow rates of the inner oil, middle aqueous, and outer oil phases are 800, 2500 and 10000 μL h^{-1}, respectively. b) Optical microscope image of the double emulsions with colloidal crystal shells after collection. c–f) Dependence of the flow rate of middle phase on the size of the double emulsions with colloidal crystal shells. The flow rate of the inner and outer oil phases is kept constant of 800 and 10000 μL h^{-1}, respectively. Optical microscope images of the double emulsions with colloidal crystal shells at the flow rate of the middle phase of c) 3000, d) 1400, and e) 500 μL h^{-1}. f) Plots of the diameter for inner drop D_i, outer drop D_o, and the thickness of colloidal crystal shell $1/2(D_o - D_i)$ as a function of the flow rate of middle phase.

After UV irradiation, the colloidal crystals in the shells can be immobilized in a polyacrylamide (PAAm) hydrogel network preserving the crystalline structure of colloids. Since the packing density of charge-stabilized colloidal crystals is adjustable, the diffraction colors or Bragg wavelength of the gel-immobilized colloidal crystal shells can be tuned easily by varying the particle concentration before gelation. For example, by evaporating water in the shells before gelation, the particle concentration, and thus the diffraction color or Bragg wavelength can be manipulated (**Figure 2**). The range of colors that can be generated is potentially useful for labeling the encapsulated materials for multiplexing. The strong reflection peak in the spectrum from the bright dot at the center of the PAAm-immobilized colloidal crystal shell is assigned to the Bragg diffraction from (111) lattice planes of a face-centered-cubic (fcc) structure aligned normal to the incident light. The detection of only 111 reflection peak suggests that the colloidal particles in the shell are well oriented parallel to the spherical interfaces as the fcc (111) lattice planes.

The diffraction color or Bragg wavelength can be altered by using a stimuli-sensitive hydrogel to immobilize the colloidal crystal. For example, colloidal crystal shell immobilized in a poly(*N*-isopropylacrylamide) (PNIPAm) gel is shown in **Figure 3**. The PNIPAm gel is a thermosensitive polymer that undergoes a volume transition at a lower critical solution temperature of ~32 °C.[17] As the temperature of the microcapsule is increased, the shell begins to shrink rapidly

© 2010 WILEY-VCH Verlag GmbH & Co. KGaA, Weinheim

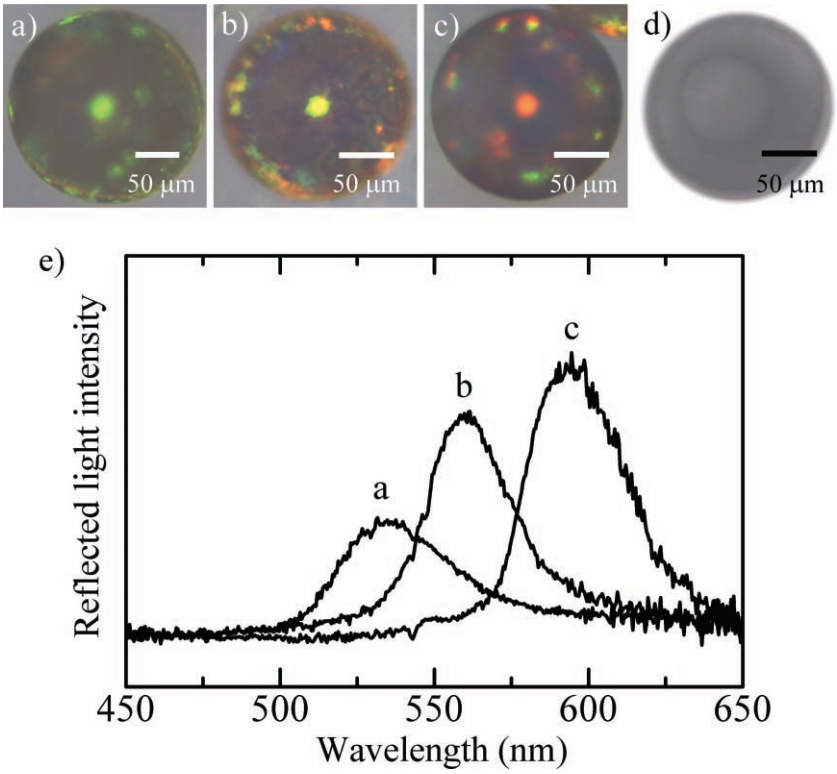

Figure 2. a–c) Photograph of the PAAm-immobilized colloidal crystal shells with the particle diameter of 198 nm and different particle concentrations under light at normal incidence. (a) ϕ_p = 0.55, b) ϕ_p = 0.45, c) ϕ_p = 0.35.) d) Photograph of the sample b under transmission light. e) Reflection spectrum at normal incidence of the PAAm-immobilized colloidal crystal shell shown in panels (a–c).

at ~32 °C, resulting in a change in the diffraction color or Bragg diffraction wavelength. Such capsules can be used as biological and chemical sensors for monitoring chemical reactions in the encapsulated materials or changes in environments through the diffraction color or Bragg diffraction wavelength.

Interestingly, the colloidal crystal shells exhibit greater sensitivity and a wider range of spectral changes compared to a bulk colloidal crystal or spherical gels of the same composition (Figure 3e). For the colloidal crystals immobilized in a conventional bulk or spherical gel, the crystal structure remains fcc during shrinkage because the lattice spacing decreases uniformly in all directions.[15] In the case of the colloidal crystal shells, the shrinkage exhibited by the inner drop is smaller than that following an isotropic shrinkage as shown in Figure 3c. This reduction in shrinkage of the inner drop is compensated by an increase in shrinkage of the gel shell in the radial direction. We believe that the PNIPAm gel shell becomes more hydrophobic and denser as the temperature increases; this leads to a decrease in its permeability to water and limits the degree to which the inner drop can shrink. Moreover, the washing step may not have completely removed all oil in the core; this can reduce the amount by which the inner drop of the colloidal crystal shell shrinks. As a result of these effects, the gel shell shrinks more in the radial direction of the gel shell as shown in Figure 3d. Thus, the lattice spacing in the radial direction undergoes greater change than that in the direction along the interfaces of the shell. The gel-immobilized colloidal crystal shell, hence, does not maintain the fcc structure during shrinkage.

The hypothesis for non-uniform changes in the lattice spacing can be corroborated by analyzing the spectral response of colloidal crystal gel shell during shrinkage. The Bragg condition of colloidal crystals for normal incidence is given by

$$\lambda = 2 n_c d_{hkl}, \quad (1)$$

where λ is the Bragg wavelength, n_c is the refractive index of the colloidal crystals, and d_{hkl} is the interplanar spacing of (hkl) lattice planes normal to the incident light. The value of n_c can be approximated by volume-weighted average of the refractive indices of the components,[18]

$$n_c = n_p \varphi_p + n_{gel} \varphi_{gel}, \quad (2)$$

where n_p and n_{gel} are the refractive indices of the polystyrene particles (n_p = 1.59) and hydrogel, respectively, and ϕ_p and ϕ_{gel} are the volume fraction of the particle and hydrogel. Since the hydrogel is composed of polymer and water, the refractive index of the hydrogel can be approximated as $n_{gel} = n_{pol}\phi_{pol}/\phi_{gel} + n_w\phi_w/\phi_{gel}$, where n_{pol} and n_w are the refractive indices of the polymer (n_{pol} = 1.50, PNIPAm) and water (n_w = 1.33), respectively, and ϕ_{pol} and ϕ_w are the volume fraction of the polymer and water. The particle volume fraction of the PNIPAm-immobilized colloidal crystal shell at each temperature can be estimated from the particle volume in the shell (8.9×10^{-13} m^3) and the shell volume determined from the diameters of inner and outer droplets (Figure 3c). The refractive indices of the crystals can be estimated by substituting the calculated particle volume fraction and the PNIPAm gel volume fraction ($\phi_{pol} = 0.16\phi_p$, which is determined from the masses of the gelation reagent and particles added into the aqueous phase) into equation (2). For colloidal crystals immobilized in the conventional bulk or spherical gel, where the crystal structure remains fcc during the shrinkage,[15] the Bragg reflection for normal incidence is caused by the lattice spacing of fcc (111) planes, which is determined from geometrical considerations using the particle volume fraction, ϕ_p and the particle diameter, d, and is given by

$$d_{111} = \left(\frac{2\pi}{9\sqrt{3}} \cdot \frac{1}{\varphi_p}\right)^{1/3} \cdot d \quad (3)$$

Assuming that the colloidal crystals in the shell gel maintains the fcc structure during the shrinkage, the Bragg wavelengths are estimated by substituting the values of d_{111} into the equation (1) and shown as open diamonds, in Figure 3e. The estimated values are in disagreement with the observed Bragg wavelengths, indicating that the colloidal crystal in the gel shell is not an fcc structure during the shrinkage. Assuming that the colloidal crystal at 22 °C is an fcc structure, we can estimate the contracted lattice

© 2010 WILEY-VCH Verlag GmbH & Co. KGaA, Weinheim

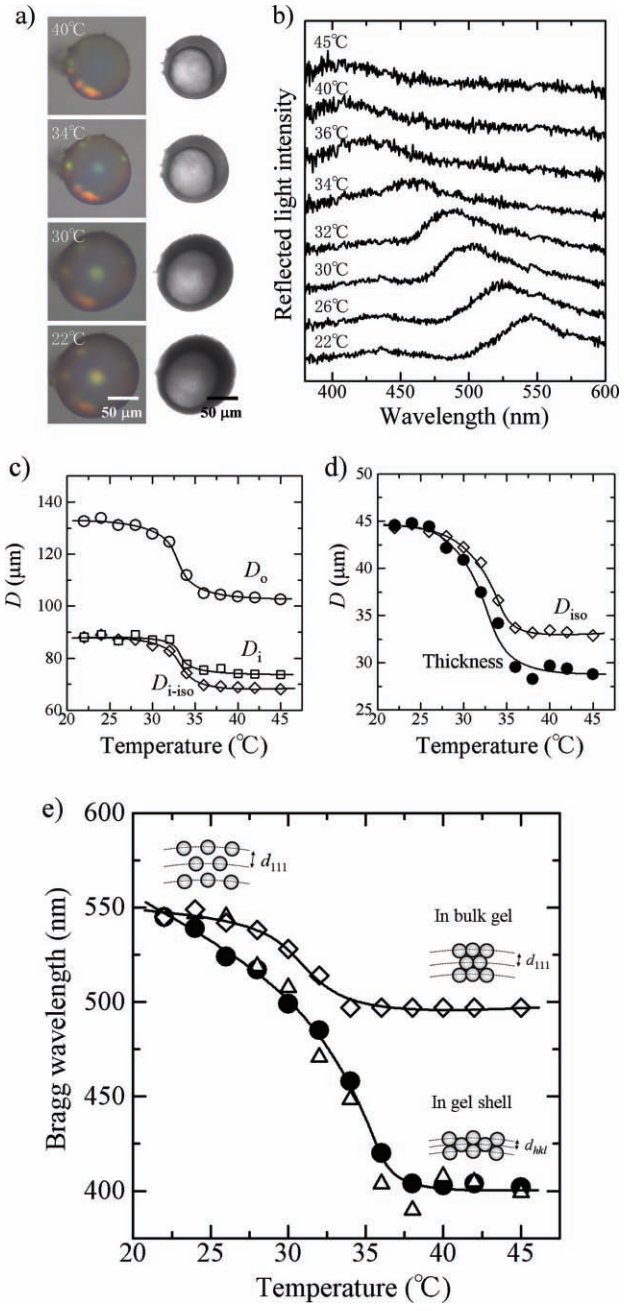

Figure 3. a) Microscopy images of the reflection and transmission at normal incidence of a thermosensitive PNIPAm-immobilized colloidal crystal shell at various temperatures. b) Reflection spectrum at normal incidence of the PNIPAm-immobilized colloidal crystal shell at various temperatures. c) Plots of the diameters of the inner drop D_i and outer drop D_o as a function of temperature. The diameter of the drop is determined from a circle with the same area. $D_{i\text{-}iso}$ is the diameter of inner drop assuming isotropic shrinkage of gel. d) Plots of the thickness of colloidal crystal shell, $1/2(D_o - D_i)$ and the shell thickness calculated assuming isotropic shrinkage of gel, D_{iso}, as a function of temperature. e) Plot of the wavelengths of Bragg reflection for the PNIPAm-immobilized colloidal crystal shell as a function of temperature. (•: experimentally measured Bragg wavelength, Δ: calculated Bragg wavelength, ◊: calculated Bragg wavelength assuming the isotropic shrinkage of gel). The curves in panels (c), (d), and (e) are guides to the eye.

spacing of planes normal to the thickness direction by using the shell thickness. By substituting the estimated lattice spacings and refractive indices into equation (1), the Bragg wavelengths are calculated and shown as open triangle in Figure 3e. The estimated values are in good agreement with the observed Bragg wavelengths. The Bragg wavelengths of the colloidal crystal shells are always smaller than those of colloidal crystals in the bulk gel; and the ultimate Bragg wavelength of the colloidal crystal shell in the most shrunken state is much smaller than that in the bulk gel. For the colloidal crystals in the conventional bulk gel, the ultimate Bragg wavelength is attained at the interplanar spacing of $d_{111} = \sqrt{\frac{2}{3}}d$, which is determined from equation (3). By contrast, the colloidal crystals immobilized in the gel shell produce a smaller interplanar spacing than that in the isotropic shrunken gel, as schematically shown in Figure 3e. Therefore, the Bragg wavelength of the colloidal crystal shell can be manipulated with higher sensitivity and over a wider range of wavelengths.

In summary, we have fabricated microcapsules with colloidal crystal shells with tunable photonic wavelengths by immobilizing charge-stabilized colloidal crystals in hydrogels. While we demonstrate the responsiveness of the colloidal crystal shell towards temperature changes, the principle should also be applicable to the fabrication of colloidal crystals that respond to changes in other stimuli, such as pH and ionic strength. Furthermore, the colloidal crystal shell would have the advantage that the reaction time to stimuli is very fast due to its thinner layer than bulk materials. Since colloidal crystals are non-toxic and are not susceptible to photo-bleaching, unlike dyes and quantum dots, these capsules are potentially useful as labels for biomolecules and as biological and chemical sensors for monitoring changes inside and outside the capsules through the Bragg diffraction wavelength or diffraction color.

Experimental Section

Microfluidics: Round glass capillary tubes (World Precision Instruments) with outer and inner diameters of 1.0 mm and 580 μm, respectively, were tapered to the desired diameter using a capillary puller (Sutter Instrument, P-97) and a microforge (Narishige, MF-830). The orifice sizes affect the dimensions of the emulsions formed, and typical dimensions of orifice for inner fluid and collection were 10 ~ 50 and 30 ~ 500 μm, respectively. The inside of the round tapered capillaries for collection was coated with a hydrophobic reagent (GELEST. Inc., Tridecafluoro-1,1,2,2-tetrahydroctyl-triethoxy silane). The tapered capillaries for inner fluid and collection were then fitted into the square capillary (Atlantic International Technology), which had an inner dimension of 1.0 mm. The distance between the capillaries for inner fluid and collection was adjusted to be 30 ~ 150 μm. A transparent epoxy resin was used to seal the tubes where required.

To generate the O/W/O double emulsions to form the microcapsules with colloidal crystal shells, we use an aqueous suspension of charged polystyrene particles; the quiescent particles form a crystalline state. Polystyrene latex (Duke Scientific Corp., particle diameter 120 or 198 nm) is deionized using a mixed-bed ion-exchange resin (Bio-Rad, AG501-X8) in vials until the suspension shows iridescence indicative of a colloidal crystal phase. To immobilize the particle arrays in hydrogel shells, the suspension is mixed with aqueous solutions of acrylamide (1 M, Sigma-Aldrich) as a monomer, *N*,*N*′-methylene-bis-acrylamide (20 mM, Fluka) as a cross-linker, and a photoinitiator (0.2 wt%, Ciba, Irgacure 2959). For fabrication of thermosensitive hydrogel shells, *N*-isopropylacrylamide (0.5 M, Sigma-Aldrich), *N*,*N*′-methylene-bis-acrylamide (10 mM), and a photoinitiator (0.2 wt%, Ciba, Irgacure 2959) are dissolved in the suspension. To stabilize the interface between the middle aqueous

© 2010 WILEY-VCH Verlag GmbH & Co. KGaA, Weinheim

phase and inner oil phase without destroying the crystalline state of the colloids, a surfactant (2–3 wt%, Tween 20) is added to the aqueous phase. The inner oil phase is a poly(dimethylsiloxane) fluid (5 cSt, Sigma-Aldrich). The outer oil phase is a poly(dimethylsiloxane) fluid (50 cSt, Sigma-Aldrich) containing a surfactant (2 wt%, Dow Corning 749) to stabilize the interface between the middle aqueous phase and outer oil phase. These solutions are filtered with 5-μm filters to remove particulate impurities and then infused into the microfluidic device through polyethylene tubing (Scientific Commodities) attached to syringes (SGE) that are driven by positive displacement syringe pumps (Harvard Apparatus, PHD 2000 series). The formation of double emulsions is monitored with a high-speed camera (Vision Research) attached to an inverted optical microscope (Leica, DMIRB). The double emulsions formed in the capillary device are irradiated by a UV lamp (UVP, UVG-54) to polymerize the gelation reagents dissolved in the middle phase. The microspheres with the polymerized colloidal crystal shells are removed from the PDMS oil and washed with 2-propanol to remove any adsorbed oil. The microspheres are then washed and stored in water.

Characterization: The normal reflection spectra of the colloidal crystal shell were measured using a fiber optic spectrometer (Ocean Optics Inc., HR2000+) attached to an optical microscope (Nikon, ECLIPSE TE2000-E). The temperature of the sample was controlled using a temperature controller (Physitemp, TS-4 ER).

Supporting Information

Supporting Information is available from the Wiley Online Library or from the author.

Acknowledgements

This work was supported by JSPS Fellowships for Research Abroad, KAKENHI (22686063), the NSF (DMR-0602684) and the Harvard MRSEC (DMR-0820484). We also thank Prof. Vinothan Manoharan and Dr. Guangnan Meng for their help with the use of spectrophotometer.

Received: June 3, 2010
Published online: August 27, 2010

[1] J.-W. Kim, A. S. Utada, A. Fernández-Nieves, Z. B. Hu, D. A. Weitz, *Angew. Chem., Int. Ed.* **2007**, *46*, 1819.
[2] D. Lee, D. A. Weitz, *Adv. Mater* **2008**, *20*, 3498.
[3] A. Fernández-Nieves, V. Vitelli, A. S. Utada, D. R. Link, M. Márquez, D. R. Nelson, D. A. Weitz, *Phys. Rev. Lett.* **2007**, *99*, 157801.
[4] a) I. T. Degim, N. Celebi, *Curr. Pharm. Des.* **2007**, *13*, 99; b) S. S. Davis, I. M. Walker, *Methods Enzymol.* **1987**, *149*, 51; c) M. Nakano, *Adv. Drug Delivery Rev.* **2000**, *45*, 1.
[5] Y. Ouyang et al., *Crit. Rev. Environ. Sci. Technol.* **1995**, *25*, 269.
[6] a) J. S. Huang, R. Varadaraj, *Curr. Opin. Colloid Interface Sci.* **1996**, *1*, 535; b) K. C. Taylor, B. F. Hawkins, In *Emulsions: Fundamental Applications in the Petroleum Industry*; (Ed: L. L. Schramm), Advances in Chemistry Series, *263*, American Chemical Society, Washington DC, **1992**.
[7] a) G. Muschiolik, *Curr. Opin. Colloid Interface Sci.* **2007**, *12*, 213; b) F. Leal-Calderon, F. Thivilliers, V. Schmitt, *Curr. Opin. Colloid Interface Sci.* **2007**, *12*, 206.
[8] a) P. Pieranski, *Contemp. Phys.* **1983**, *24*, 25; b) *Ordering and Phase Transitions in Charged Colloids*, (Eds: A. K. Arora, B. V. R. Tata), VCH, New York **1996**; c) K. Ito, K. Sumaru, N. Ise, *Phys. Rev. B* **1992**, *46*, 3105; d) T. Kanai, T. Sawada, A. Toyotama, K. Kitamura, *Adv. Funct. Mater.* **2005**, *15*, 25.
[9] a) Special Issue on Photonic Crystals, *Adv. Mater.* **2001**, *13*, 369; b) E. Yablonovitch, *Phys. Rev. Lett.* **1987**, *58*, 2059; c) S. John, *Phys. Rev. Lett.* **1987**, *58*, 2486; d) J. D. Joannopoulos, R. D. Meade, J. N. Winn, *Photonic Crystals*, Princeton University Press, Princeton, NJ,**1995**; e) A. van Blaaderen, R. Ruel, P. Wiltzius, *Nature* **1997**, *385*, 321.
[10] a) E. A. Kamenetzky, L. G. Magliocco, H. P. Panzer, *Science* **1994**, *263*, 207; b) S. H. Foulger, P. Jiang, A. Lattam, D. W. Smith, J. Ballato, D. E. Dausch, S. Grego, B. R. Stoner, *Adv. Mater.* **2003**, *15*, 685; c) A. Toyotama, T. Kanai, T. Sawada, J. Yamanaka, K. Ito, K. Kitamura, *Langmuir* **2005**, *21*, 10268.
[11] a) Y. Iwayama, J. Yamanaka, Y. Takiguchi, M. Takasaka, K. Ito, T. Shinohara, T. Sawada, M. Yonese, *Langmuir* **2003**, *19*, 977; b) H. Fudouzi, T. Sawada, *Langmuir* **2006**, *22*, 1365; c) T. Kanai, T. Sawada, A. Toyotama, J. Yamanaka, K. Kitamura, *Langmuir* **2007**, *23*, 3503.
[12] J. R. Lawrence, Y. Ying, P. Jiang, S. H. Foulger, *Adv. Mater.* **2006**, *18*, 300.
[13] a) J. Holtz, S. A. Asher, *Nature* **1997**, *389*, 829; b) H. Saito, Y. Takeoka, M. Watanabe, *Chem. Commun.* **2003**, 2126.
[14] a) A. S. Utada, E. Lorenceau, D. R. Link, P. D. Kaplan, H. A. Stone, D. A. Weitz, *Science* **2005**, *308*, 537; b) R. K. Shah, H. C. Shum, A. C. Rowat, D. Lee, J. J. Agresti, A. S. Utada, L. Y. Chu, J.-W. Kim, A. Fernandez-Nieves, C. J. Martinez, D. A. Weitz, *Mater. Today* **2008**, *11*, 18; c) H. C. Shum, J.-W. Kim, D. A. Weitz, *J. Am. Chem. Soc.* **2008**, *130*, 9543.
[15] T. Kanai, D. Lee, H. C. Shum, D. A. Weitz, *Small* **2010**, *6*, 807.
[16] a) S.-H. Kim, S.-J. Jeon, S.-M. Yang, *J. Am. Chem. Soc.* **2008**, *130*, 6040; b) S.-H. Kim, J.-M. Lim, W. C. Jeong, D.-G. Choi, S.-M. Yang, *Adv. Mater.* **2008**, *20*, 3211; c) V. Rastogi, S. Melle, O. G. Calderón, A. A. García, M. Marquez, O. D. Velev, *Adv. Mater.* **2008**, *20*, 4263.
[17] a) B. R. Saunders, B. Vincent, *Adv. Colloid Interface Sci.* **1999**, *80*, 1; b) R. K. Shah, J. W. Kim, J. J. Agresti, D. A. Weitz, *Soft Matter* **2008**, *12*, 2303.
[18] P. A. Hiltner, I. M. Krieger, *J. Phys. Chem.* **1969**, *73*, 2386.

© 2010 WILEY-VCH Verlag GmbH & Co. KGaA, Weinheim